



This discussion paper is/has been under review for the journal Atmospheric Chemistry and Physics (ACP). Please refer to the corresponding final paper in ACP if available.

# Organic photolysis reactions in tropospheric aerosols: effect on secondary organic aerosol formation and lifetime

A. Hodzic<sup>1</sup>, S. Madronich<sup>1</sup>, P. S. Kasibhatla<sup>2</sup>, G. Tyndall<sup>1</sup>, B. Aumont<sup>3</sup>,  
J. L. Jimenez<sup>4</sup>, J. Lee-Taylor<sup>1</sup>, and J. Orlando<sup>1</sup>

<sup>1</sup>National Center for Atmospheric Research, Boulder, CO, USA

<sup>2</sup>Nicholas School of the Environment, Duke University, Durham, USA

<sup>3</sup>LISA UMR CNRS 7583, Université Paris Est Créteil et Université Paris Diderot, France

<sup>4</sup>University of Colorado, Boulder, CO, USA

Received: 18 February 2015 – Accepted: 26 February 2015 – Published: 17 March 2015

Correspondence to: A. Hodzic (alma@ucar.edu)

Published by Copernicus Publications on behalf of the European Geosciences Union.

Title Page

Abstract

Introduction

Conclusions

References

Tables

Figures



Back

Close

Full Screen / Esc

Printer-friendly Version

Interactive Discussion



## Abstract

This study presents the first modeling estimates of the potential effect of gas- and particle-phase organic photolysis reactions on the formation and lifetime of secondary organic aerosols (SOA). Typically only photolysis of smaller organic molecules (e.g. formaldehyde) for which explicit data exist is included in chemistry-climate models. Here, we specifically examine the photolysis of larger molecules that actively partition between the gas and particle phases. The chemical mechanism generator GECKO-A is used to explicitly model SOA formation from  $\alpha$ -pinene, toluene, and C<sub>12</sub> and C<sub>16</sub> *n*-alkane reactions with OH at low- and high-NO<sub>x</sub>. Simulations are conducted for typical mid-latitude conditions and a solar zenith angle of 45° (permanent daylight). The results show that after four days of chemical aging under those conditions (equivalent to eight days in the summer mid-latitudes), gas-phase photolysis leads to a moderate decrease in SOA yields i.e. ~ 15 % (low-NO<sub>x</sub>) to ~ 45 % (high-NO<sub>x</sub>) for  $\alpha$ -pinene, ~ 15 % for toluene, ~ 25 % for C<sub>12</sub>-alkane, and ~ 10 % for C<sub>16</sub>-alkane. The small effect on low volatility *n*-alkanes such as C<sub>16</sub>-alkane is due to the rapid partitioning of early-generation products to the particle phase where they are assumed to be protected from gas-phase photolysis. Minor changes are found in the volatility distribution of organic products and in oxygen to carbon ratios. The decrease in SOA mass seems increasingly more important after a day of chemical processing, suggesting that most laboratory experiments are likely too short to quantify the effect of gas-phase photolysis on SOA yields. Our results also suggest that many molecules containing chromophores are preferentially partitioned into the particle phase before they can be photolyzed in the gas-phase. Given the growing experimental evidence that these molecules can undergo in-particle photolysis, we performed sensitivity simulations using an estimated SOA photolysis rate of  $J_{\text{SOA}} = 4 \times 10^{-4} J_{\text{NO}_2}$ . Modeling results indicate that this photolytic loss rate would decrease SOA mass by 40–60 % for most species after ten days of equivalent atmospheric aging at mid-latitudes in the summer. It should be noted that in our simulations we do not consider in-particle or aqueous-phase reactions which

ACPD

15, 8113–8149, 2015

## Organic photolysis reactions in tropospheric aerosols

A. Hodzic et al.

Title Page

Abstract

Introduction

Conclusions

References

Tables

Figures

◀

▶

◀

▶

Back

Close

Full Screen / Esc

Printer-friendly Version

Interactive Discussion



could modify the chemical composition of the particle, and thus the amount of photolabile species. The atmospheric implications of our results are significant for both the SOA global distribution and lifetime. GEOS-Chem global model results suggest that particle-phase photolytic reactions could be an important loss process for SOA in the atmosphere, removing aerosols from the troposphere on timescales (less than 7 days) that are comparable to wet deposition.

## 1 Introduction

Secondary organic aerosols (SOA) are ubiquitous atmospheric constituents formed by photochemical oxidation of anthropogenic and biogenic hydrocarbons that can lead to adverse health effects (Fann et al., 2012) and radiative forcing of climate (Boucher et al., 2013). Their atmospheric burden and lifetime are highly uncertain due to our limited understanding of processes controlling their formation, aging and removal in the atmosphere. SOA yields and the volatility distribution of intermediate oxidation products greatly depend on the competitive chemistry of peroxy radicals ( $\text{RO}_2$ ) formed from oxidation of parent hydrocarbons, which can react with nitrogen oxides (NO), hydroperoxy radicals ( $\text{HO}_2$ ), or other  $\text{RO}_2$  (Ziemann and Atkinson, 2012). The resulting oxygenated molecules contain carbonyl, peroxide or nitrate chromophores, and are potentially sensitive to photolysis during their lifetime in the atmosphere (Finlayson-Pitts and Pitts, 2000). Photolysis can occur in the gas-phase and in the condensed phase as particles containing photolabile compounds efficiently absorb light at actinic wavelengths (e.g. Lambe et al., 2013; Wong et al., 2014). Unlike OH reactions that mainly lead to addition of more functional groups, photolysis mainly fragments molecules into smaller and more volatile compounds thus significantly modifying SOA composition and properties during atmospheric aging.

Evidence that photolysis modulates SOA formation and lifetime in the atmosphere is supported by a growing number of laboratory experiments, which showed that exposure to UV lights can suppress SOA formation or even cause substantial loss of

Title Page

Abstract

Introduction

Conclusions

References

Tables

Figures



Back

Close

Full Screen / Esc

Printer-friendly Version

Interactive Discussion



**Organic photolysis reactions in tropospheric aerosols**

A. Hodzic et al.

Title Page

Abstract

Introduction

Conclusions

References

Tables

Figures

◀

▶

◀

▶

Back

Close

Full Screen / Esc

Printer-friendly Version

Interactive Discussion

biogenic SOA. Presto et al. (2005) observed a 20–40 % decrease in aerosol yields during  $\alpha$ -pinene ozonolysis experiments conducted under UV lights. Zhang et al. (2006) found similar sensitivity to UV exposure for d-limonene ozonolysis SOA, with a mass yield decrease of 60 % for compounds with saturation concentration of  $1 \mu\text{g m}^{-3}$ . In both cases, the SOA decrease was attributed to the photolysis of gas-phase intermediates during the active growth phase and changes in their volatility distribution. Specific SOA aging experiments were also performed to isolate the effect of photolysis from other processes (e.g. Tritscher et al., 2011; Salo et al., 2011; Henry and Donahue, 2012; Donahue et al., 2012). In those experiments, SOA was first formed from  $\alpha$ -pinene ozonolysis in the dark, and then the products were irradiated (with UV lamps or solar lights), which allowed separation of the aging by OH-radical oxidation and photolysis from the initial condensation of primary products. Henry and Donahue (2012) reported a strong photolytic loss of  $6 \times 10^{-5} \text{ s}^{-1}$  of the formed SOA mass upon UV 360 nm black-light exposure with lower OH levels ( $\sim 10^6 \text{ molecules cm}^{-3}$ ) via  $\text{H}_2\text{O}_2$  photolysis. In additional experiments reported by Donahue et al. (2012), where OH was formed via HONO photolysis, an initial increase in SOA concentrations was first observed, followed by their strong decrease as OH concentrations dropped from  $10^7$  to  $10^6 \text{ molecules cm}^{-3}$ . The authors attributed this SOA loss to photolysis in the gas-phase followed by particle-to-gas re-equilibration, under the assumption that particle-phase quantum yields of photodissociation are small due to quenching and cage effects from neighboring molecules. However, recent studies that were able to decouple gas-phase and condensed-phase processes seem to suggest a rapid photolytic loss of SOA in the condensed phase. Epstein et al. (2014) irradiated  $\alpha$ -pinene ozonolysis SOA denuded from gas-phase oxidants and organic vapors, and concluded that condensed-phase photolysis was responsible for a significant decrease in SOA mass caused by the photochemical loss of particle-bound peroxide species (a 50 % loss over 1 week in the atmosphere). Wong et al. (2014) also reported a substantial photolytic loss of  $\alpha$ -pinene SOA mass (generated by re-atomization after sampling into filters)

under UVB lights with loss rates of  $7.9 \times 10^{-5} \text{ s}^{-1}$  under dry conditions and a 2x faster loss ( $1.6 \times 10^{-4} \text{ s}^{-1}$ ) under higher relative humidities.

During photochemical aging in the atmosphere, SOA can be both generated by oxidative functionalization with OH, and destroyed by photolysis. As these processes are occurring simultaneously and during the entire organic aerosol (OA) lifecycle in the atmosphere (typically a week), it is currently challenging to quantify separately the effect of photolysis on SOA yields and aging from laboratory experiments, and to describe their effect in the models. To our knowledge, photolysis of oxygenated organic molecules in the gas or condensed phase is ignored in most current chemistry-climate models, which could result in substantial errors in SOA predictions. In addition, the experimental quantification of SOA photolytic loss could be significantly biased due to SOA evaporation caused by heating inside the chamber upon UV light exposure (Denjean et al., 2014).

The objective of the present study is to examine the effect of both gas- and condensed-phase photolysis on SOA formation and lifetime using process and global modeling. First, the role of photolysis on the multi-day growth of SOA is studied for four typical precursors including  $\alpha$ -pinene, toluene, and semi-volatile and intermediate volatility *n*-alkanes. The mechanism generator GECKO-A is used to create explicit oxidation schemes for these precursors, which are then run within a box model to assess the effect of photolysis on SOA yields under a range of conditions. The effect of gas-phase photolysis is explicitly quantified in the model, whereas the potential role of in-particle photolysis is estimated by two different methods and discussed based on sensitivity simulations. Finally, a simplified parameterization of photolysis reactions is included within a global chemistry model to estimate their potential effect on the global SOA distribution.

**Organic photolysis reactions in tropospheric aerosols**

A. Hodzic et al.

Title Page

Abstract

Introduction

Conclusions

References

Tables

Figures



Back

Close

Full Screen / Esc

Printer-friendly Version

Interactive Discussion



## 2 Modeling framework

The mechanism self-generator GECKO-A (Generator of Explicit Chemistry and Kinetics of Organics in the Atmosphere) was used in this study to create the detailed gas-phase oxidation mechanisms for individual SOA precursors including  $\alpha$ -pinene, toluene, and  $C_{12}$  and  $C_{16}$   $n$ -alkanes. The chemical mechanisms are created using a prescribed set of rules determining reaction pathways and rate coefficients, based on laboratory kinetic data, and structure–activity relationships as described by Aumont et al. (2005). The protocol currently implemented in GECKO-A allows the generation of chemical mechanisms for aliphatic species only. For aromatic species (i.e. toluene in this study), the mechanism is taken from the Master Chemical Mechanism (MCM) (Jenkin et al., 2003) up to the formation of open ring products, beyond which the mechanism generated by GECKO-A is used. Rate coefficients for reaction of OH with organics are based on structure-reactivity rules of Kwok and Atkinson (1995) and subsequent updates. In this study, we have updated the rate constants for H-atom abstraction from carbon atoms containing a hydroperoxide functionality (e.g., RC-H(OOH)R). Kinetic data for OH/hydroperoxide reactions are sparse in the literature, and previous versions of GECKO-A assumed an activation factor of 14 on the basis of data for the OH/CH<sub>3</sub>OOH reaction. That is, the presence of the –OOH group was assumed to increase the reactivity of the adjacent C-H bond(s) by this factor. We have changed this factor to 3.5 similar to that for –OH (Atkinson R., personal communication, 2015), and discuss its effect on our results in Sect. 3.1. The choice of a lower activation factor is supported by measurements of gas-phase dodecyl hydroperoxides in the work of Yee et al. (2012), who found that the loss of these peroxides was much too fast when using the MCM value based on a large value of F(-OOH). For the gas-particle partitioning, instantaneous equilibrium is assumed, and the Nannoolal et al. (2008) approach is used to estimate the saturation vapor pressure for non-radical species. The fraction that is partitioned to the particle phase can be determined as  $F_{\text{aerosol}, i} = \left( \frac{C_{\text{OA}}}{C_{\text{OA}} + C_i^*} \right)$  where  $C_{\text{OA}}$  is the aerosol mass concentration ( $\mu\text{g m}^{-3}$ ), and  $C_i^*$  is an effective saturation mass con-

[Title Page](#)[Abstract](#)[Introduction](#)[Conclusions](#)[References](#)[Tables](#)[Figures](#)[Back](#)[Close](#)[Full Screen / Esc](#)[Printer-friendly Version](#)[Interactive Discussion](#)

centration ( $\mu\text{g m}^{-3}$ ). The gas/particle equilibrium and the composition of SOA are constantly modified as the gas-phase oxidation progresses during the atmospheric aging. Condensed-phase reactions are not considered, nor are potential diffusion limitations to SOA partitioning. Gas-phase photolytic reactions are included for molecules containing carbonyl, hydroperoxide or nitrate chromophores. For species containing several functional groups, each chromophore is treated independently, except for conjugated carbonyls. The photolysis of nitroaromatic compounds is not included. To determine the associated photolysis rates, each molecular structure predicted by GECKO-A is assigned a reference compound with its associated cross sections and quantum yields as described by Aumont et al. (2005, see Table 4). SI-Table 1 summarizes the photolysis rates for chromophores and molecular structures that are considered in GECKO-A. Particle-phase photolysis is not explicitly calculated in the default model, and sensitivity simulation are performed in this study to quantify its effects as discussed in Sect. 3.2.

In this study, simulations are performed in a box model with the prescribed conditions representative of ambient air as in the study by Hodzic et al. (2014) to quantify the effect of photolysis on SOA formation and yields. In these runs, temperature is set to 298 K, photolysis frequencies are calculated for mid-latitudes at a solar zenith angle of  $45^\circ$  ( $J_{\text{NO}_2} = 8.1 \times 10^{-3} \text{ s}^{-1}$ ),  $\text{NO}_x$  levels are held at 0.01 ppb for low and 10 ppb for high- $\text{NO}_x$  conditions, ozone is set at 40 ppb, and OH is kept constant at  $2 \times 10^6 \text{ molecules cm}^{-3}$ . The pre-existing OA concentration is  $10 \mu\text{g m}^{-3}$ , typical of moderately polluted conditions. Sensitivity simulations with higher OH values ( $8 \times 10^6 \text{ molecules cm}^{-3}$ ) or lower pre-existing OA ( $1 \mu\text{g m}^{-3}$ ) are also performed. The initial hydrocarbon mixing ratio is fixed to an arbitrary low value of 1 ppt, so that the amount of aerosol produced from the given precursor is negligible compared to preexisting OA prescribed in the study and will not impact the gas/particle partitioning, nor the overall photochemical reactivity. Under these conditions, SOA yields are independent of the amount of initial precursor as discussed by Hodzic et al. (2014). SOA yields and volatility distribution of intermediate products depend to a large extent on the relative rates of  $\text{RO}_2 + \text{HO}_2$  and  $\text{RO}_2 + \text{RO}_2$

**Organic photolysis reactions in tropospheric aerosols**

A. Hodzic et al.

Title Page

Abstract

Introduction

Conclusions

References

Tables

Figures

◀

▶

◀

▶

Back

Close

Full Screen / Esc

Printer-friendly Version

Interactive Discussion











**Organic photolysis  
reactions in  
tropospheric  
aerosols**

A. Hodzic et al.

Title Page

Abstract

Introduction

Conclusions

References

Tables

Figures



Back

Close

Full Screen / Esc

Printer-friendly Version

Interactive Discussion



formed to evaluate these effects (Fig. 1). As expected, SOA formation occurs more rapidly when a 4-fold increase in OH is considered. The decrease by an order of magnitude in the amount of the pre-existing OA (and thus reduced gas/particle partitioning) also affects the amount of SOA formed. A large ( $\sim 75\%$ ) decrease in SOA production is observed for toluene because a significant fraction of the predicted oxidation products have effective saturation mass concentrations ( $C^*$ ) in the  $1\text{--}10^3\ \mu\text{g m}^{-3}$  range (Fig. 4, see also Hodzic et al., 2014). The effect is more limited for SOA produced from other precursors (up to 30%). For all precursor species, the sensitivity to photolytic reactions remains qualitatively similar (within 10%) regardless of the OH and OA background values (Figure SI-1). As expected, a decrease in background OA concentrations leads in most cases to an enhancement of the SOA photolytic loss, whereas an increase in OH levels tends to result in a reduced SOA photolytic removal.

Figure 2 shows the major functional groups in SOA molecules from various precursors. Fifteen families of functional groups are considered and they account for 54 to 65% of the total SOA mass for  $\alpha$ -pinene, 94 to 99% for toluene, and for 70 to 90% for  $C_{12}$  and  $C_{16}$  *n*-alkanes. Positional isomers are lumped into the same family of compounds. Ketone (K) and alcohol (O) moieties are present in a majority of the molecules, while hydroperoxides (H) are seen mainly at low  $\text{NO}_x$  and nitrates (N) mainly at high  $\text{NO}_x$ . Gas-phase photolysis leads to a decrease in most species, which seems to be particularly important for highly functionalized compounds containing multiple carbonyl and nitrate groups (e.g. HKKKK, HHKK, HHKKK, HKKK, NNKK, NNKO). These species are formed by several generations of chemistry and are mainly found in the particle-phase. Thus their decrease is more likely related to reductions in their precursor species due to photodegradation than to their direct loss by gas-phase photolysis. Some molecules containing alcohol groups (e.g. HHO, HKKO, HHKO) see an increase in their concentrations due to gas-phase photolysis (see also Fig. SI-2). This increase can be explained by photolysis of hydroperoxides, which can lead to the formation of alkoxy radicals that can isomerize to form alcohols. Thus photolysis can both contribute to SOA loss and to a lesser extent to its formation. Typically, photolysis of

**Organic photolysis reactions in tropospheric aerosols**

A. Hodzic et al.

Title Page

Abstract

Introduction

Conclusions

References

Tables

Figures

◀

▶

◀

▶

Back

Close

Full Screen / Esc

Printer-friendly Version

Interactive Discussion



carbonyl compounds (ketone and aldehydes) tends to break the  $\alpha$ -carbon bond on either side of the C=O group, leading to smaller more volatile fragments, that are less likely to partition to the particle phase. On the other hand, photolysis of hydroperoxides and nitrates leads to elimination of -OH or -NO<sub>2</sub>, leading to alkoxy radicals, and potentially further functionalization of the carbon skeleton favoring formation of less volatile organic compounds, that can partition more readily to the particle.

One of the highly uncertain factors that can influence the composition of SOA at low-NO<sub>x</sub> is the choice of the rate for abstracting the H atoms from the carbon atom that is adjacent to the hydroperoxide (-OOH) group. As discussed in Sect. 2, in this paper we have used a lower activation value of 3.5 for estimating the rate constant of that process, instead of the GECKO-A default value of 14 (Aumont et al., 2005). As shown in Figure SI-3 this change does not affect the SOA production when the gas-phase photolysis of organics is turned off ( $\sim 8 \mu\text{g m}^{-3}$  for C<sub>12</sub> *n*-alkane). However, the composition of SOA formed from *n*-alkanes is significantly modified, as is the effect of gas-phase photolysis on SOA yields ( $\sim 2\times$  smaller when the value of 3.5 is considered). The main difference is found for HKKKK and HKKK molecules which are much more abundant when the value of 14 is used. These molecules originate typically from successive OH reactions, leading to hydroperoxide moieties under low-NO<sub>x</sub> conditions and their subsequent fast oxidation to a ketone moiety due to a the large activation factor used. Reducing this factor to 3.5 forces the OH to react away from the -OOH group. When the carbon backbone is sparsely functionalized, this increases the rate of production of multifunctional species, in particular multifunctional peroxydes (e.g. HHO et HHK). However, when the carbon backbone is highly functionalized, this leads to more fragmentation, because in most cases the OH attack is now next to other functional moieties (e.g. multifunctional ketones).

Figure 3 shows the effect of gas-phase photolysis on oxygen to carbon (O/C) ratios of particles for the BASE run. For all cases, changes in O/C ratios ( $< 0.05$ ) are minor. Slightly higher O/C ratios at low NO<sub>x</sub> were found in the presence of gas-phase photolysis as photolyzed fragments are typically smaller and more volatile carbon chains that

**Organic photolysis reactions in tropospheric aerosols**

A. Hodzic et al.

Title Page

Abstract

Introduction

Conclusions

References

Tables

Figures



Back

Close

Full Screen / Esc

Printer-friendly Version

Interactive Discussion



need to undergo further oxidation to condense into particles. Our results are consistent with chamber studies by Wong et al. (2014) that observed small changes in O/C with an increase in more oxidized compounds (high O/C) in  $\alpha$ -pinene SOA due to fast photodegradation of less oxidized particulate organics such as carbonyls. Changes in SOA composition due to gas-phase photolysis can also affect the volatility distribution of oxidized organic compounds. Figure 4 does not show a clear shift in volatility due to gas-phase photolysis, but rather suggests that the SOA reduction is happening across a wide range of volatility bins.

Our explicit modeling results suggest that gas-phase photolysis leads in some cases to moderate changes in SOA yields (< 25 % for most precursors; < 45 % for high-NO<sub>x</sub>  $\alpha$ -pinene), and small changes in volatility distribution and O/C ratios over 1 equivalent week of chemical aging in the mid-latitude atmosphere in summer or 3 weeks in winter. The implication in terms of SOA atmospheric lifetime is that gas-phase photolysis is a possible sink of intermediate organic vapors and thus SOA, although a smaller sink compared to dry deposition of these gaseous species (Hodzic et al., 2014; Knote et al., 2014). Indeed, the estimated summertime atmospheric lifetimes against photolysis of the SOA from the four precursors considered in our study range from about 10 days for  $\alpha$ -pinene under high-NO<sub>x</sub> conditions (unlikely case), to more than a month for  $\alpha$ -pinene under low-NO<sub>x</sub> conditions or for long chain *n*-alkane species. These lifetimes are considerably longer than values reported by laboratory studies (e.g. Henry and Donahue, 2012). Current 3-D models typically represent the oxidation products as lumped surrogate species based on their volatility that can further age by OH oxidation but cannot photolyze due to the undefined chemical structure of those intermediate species. Our results suggest that omitting their gas-phase photolysis will likely result in reasonably small biases in SOA predictions over urban scales. However, errors could be significant at the global scale in particular in the upper troposphere where models have the tendency to accumulate SOA due to a less efficient wet removal.

## 3.2 Importance of in-particle photolysis of organics

In the GECKO-A simulations described above, once the organic molecules are partitioned to SOA they are protected from gas-phase photolysis. However, these molecules still contain numerous chromophores (Fig. 2) that absorb solar radiation, and could undergo photolysis inside the particle. Optical absorption is also likely to be modified by the heterogeneous formation of high molecular weight compounds inside the particle (Graber and Rudich, 2006). As GECKO-A does not include condensed-phase photochemical reactions (or heterogeneous chemistry), the effect of particle-phase photolysis on SOA cannot be calculated directly. In this section we apply two simple approaches to examine the potential effect of particle-phase photolysis within GECKO-A.

In the first approach, we assume that all organic molecules can photolyze in both gas and particle phases in GECKO-A at the gas-phase rate coefficient. This corresponds to assuming that not only are chromophores similar in their gas- and particle-phase absorption (i.e. neglecting possible effects from hydration or oligomerization), but also that the quantum yields are the same in the two phases (i.e. neglecting cage and quenching effects). These are clearly crude assumptions, but provide a framework for estimating sensitivity to these various parameters. Radical species that are produced by photolysis inside the particle are partitioned back to the gas-phase where in one case ( $J_{\text{molec}}$ ) they can undergo further chemistry and possibly repartition to the aerosol after further functionalization, or be permanently lost to the gas-phase ( $J_{\text{molecmax}}$ ). Both simulations are performed for all precursors considered here except for  $\alpha$ -pinene where for reasons of numerical stiffness only  $J_{\text{molecmax}}$  was considered. In all cases the estimated effects should be considered as an upper limit as the caging effects inside the particle are expected to increase the collision rates of these radicals within the particle and prevent them from escaping. Our results show a substantial decrease in SOA concentrations for most species (Figs. 5 and SI-1). The equivalent atmospheric lifetime of SOA with this upper limit of particle-phase photolysis was estimated to be relatively short for  $\alpha$ -pinene SOA ( $< 4$  days,  $J_{\text{molecmax}}$ ), low- $\text{NO}_x$  toluene SOA ( $\sim 4$  days,  $J_{\text{molec}}$ ),  $\text{C}_{12}$   $n$ -

[Title Page](#)[Abstract](#)[Introduction](#)[Conclusions](#)[References](#)[Tables](#)[Figures](#)[Back](#)[Close](#)[Full Screen / Esc](#)[Printer-friendly Version](#)[Interactive Discussion](#)

## Organic photolysis reactions in tropospheric aerosols

A. Hodzic et al.

Title Page

Abstract

Introduction

Conclusions

References

Tables

Figures

◀

▶

◀

▶

Back

Close

Full Screen / Esc

Printer-friendly Version

Interactive Discussion



alkane SOA (8–14 days,  $J_{\text{molec}}$ ) and high- $\text{NO}_x$   $\text{C}_{16}$   $n$ -alkane SOA ( $\sim 14$  days). These results show that a large fraction of molecules containing chromophores were partitioned into the particle phase before they could be photolyzed in the gas-phase. The difference between  $J_{\text{molecmax}}$  and  $J_{\text{molec}}$  simulations suggests that for toluene most of the photolyzed molecules stay permanently in the gas-phase, whereas for less volatile compounds such as  $\text{C}_{16}$   $n$ -alkane most of the photolyzed species undergo further gas-phase chemistry which leads to more functionalized species that can partition back to the particle phase.

We note here that in-particle reactions are not included, and are likely to modify the chemical composition of the particle, and therefore change the amount of photolabile species. For example, the work of Yee et al. (2012) and Schilling-Fahnestock et al. (2014) indicate extensive formation of peroxyhemiacetals in the SOA from dodecane oxidation at low  $\text{NO}_x$ . However, the precursor molecules are third and fourth generation products, which contain additional, unfunctionalized ketone groups, which would still be susceptible to photolysis.

In the second approach we base our estimates of condensed-phase photolysis on measured SOA mass absorption coefficient (MAC). Organic particles containing photolabile compounds have been shown to efficiently absorb light at actinic wavelengths. Recently measured MAC values range from 0.03 to  $0.5 \text{ m}^2 \text{ g}^{-1}$  for laboratory data (Lambe et al., 2013) or from 0.1 to  $10 \text{ m}^2 \text{ g}^{-1}$  for ambient urban measurements (e.g. Barnard et al., 2008) in the 300–400 nm wavelength interval. We use those measurements to estimate the condensed-phase photolysis of SOA. We represent the photolytic SOA loss as a first order reaction, with effective reaction rate coefficient  $J_{\text{SOA}}$  scaled to known  $\text{NO}_2$  photolysis:

$$J_{\text{SOA}} = J_{\text{NO}_2} \times [\text{AF}/J_{\text{NO}_2}] \times [\text{MAC}] \times [m_c] \times [\text{QY}] \quad (1)$$

where AF is the actinic flux ( $\text{photons m}^{-2} \text{ s}^{-1}$ ), MAC is the SOA mass absorption coefficient ( $\text{m}^2 \text{ g}^{-1}$ ),  $m_c$  is the mass of one carbon atom (g) and QY is the quantum yield or the probability that absorbed photons will lead to bond cleavage and

the loss of some mass from the particle. We assume that if each absorbed photon leads to the loss of one C atom, the quantum yield is equal to one. The photolysis model TUV (v5.1, Madronich et al., 1993) was used to estimate the UV actinic flux ( $= 2 \times 10^{20}$  photons  $\text{m}^{-2} \text{s}^{-1}$ ) and  $\text{NO}_2$  photolysis ( $= 9.7 \times 10^{-3} \text{s}^{-1}$ ) over 280–400 nm at 1 km altitude and overhead sun. The resulting SOA photolysis rate can be written as:

$$J_{\text{SOA}} = 0.4 \times J_{\text{NO}_2} \times [\text{MAC}] \times [\text{QY}] \quad (2)$$

To estimate the plausible range of  $J_{\text{SOA}}$  values, we use the combinations of  $[\text{MAC}] \times [\text{QY}]$  reported in the literature. Here we use MAC of  $0.1 \text{m}^2 \text{g}^{-1}$  as a lower limit for ambient aerosols. QY has only been measured for a handful of species. Calvert and Pitts (1966) reported values of 0.01 (or 1%) for photolysis of aldehydes in the aqueous phase. Lignell et al. (2013) reported values of 0.5 for cis-pinonic acid, which is one of the constituents of  $\alpha$ -pinene SOA, whereas Wong et al. (2014) estimated the quantum yield of 1.2 for the loss of organics in the case of  $\alpha$ -pinene SOA photolysis. Given the range of values, here we use a conservative value of 0.01 (or 1%) for QY. Thus our best estimate for  $J_{\text{SOA}}$  is 0.04% of  $J_{\text{NO}_2}$ . We note that this calculated value is 1–2 order of magnitude lower than those reported by Henry and Donahue (2012) who estimated the photolytic loss of SOA as 2% of  $J_{\text{NO}_2}$  (total value of both particle and gas-phase photolysis and  $J_{\text{NO}_2}$  of  $3 \times 10^{-3} \text{s}^{-1}$ ). In their experiments, Henry and Donahue (2012) argued that photolysis is more efficient (higher QY) in the gas-phase than in the particle phase where quenching and caging are more likely to occur and could cause rapid recombination of fragments. Therefore a lower QY may be expected in the particles, although it is unclear whether similar molecules are involved in photolysis in the two phases. We also note that photolysis of SOA is assumed to not occur at visible wavelengths (i.e.  $\text{QY} = 0$  for  $\lambda > 400 \text{nm}$ ).

Figure 5 shows that considering the above estimated condensed-phase photolytic loss of SOA ( $J_{\text{SOA}} = 4 \times 10^{-4} \times J_{\text{NO}_2} = 3.2 \times 10^{-6} \text{s}^{-1}$ ; lifetime of 7 days at equivalent  $J_{\text{NO}_2}$  atmospheric exposure, see Table 1) in GECKO-A simulations leads to a 40–60% decrease in SOA mass after ten days of equivalent atmospheric aging for most species

## Organic photolysis reactions in tropospheric aerosols

A. Hodzic et al.

[Title Page](#)[Abstract](#)[Introduction](#)[Conclusions](#)[References](#)[Tables](#)[Figures](#)[⏪](#)[⏩](#)[◀](#)[▶](#)[Back](#)[Close](#)[Full Screen / Esc](#)[Printer-friendly Version](#)[Interactive Discussion](#)



( $J_{\text{mac}}$  run, Figs. 2 and SI-1). A more limited decrease (15%) is found for the high- $\text{NO}_x$  toluene SOA because the photolytic loss of nitroaromatic compounds, which are predicted to be the major SOA constituents (RVVO in Fig. 2), is not included. The comparison between  $J_{\text{mac}}$  and  $J_{\text{molec}}$  shows a fairly similar (within 20%) reduction in SOA mass for most precursors. In the case of low- $\text{NO}_x$   $\text{C}_{16}$   $n$ -alkane SOA,  $J_{\text{mac}}$  resembles  $J_{\text{molecmax}}$  suggesting that considering further gas-phase chemistry of photolysis fragments might be important for low volatility species. However, these compounds could become sensitive to photolysis if e.g. heterogeneous chemistry occurred inside the particle and modified its chemical composition.

The overall SOA loss rate due to the combined effect of gas- and particle-phase photolysis (and ongoing OH chemistry) in GECKO-A runs was estimated for the  $J_{\text{mac}}$  simulations (see Table 4). Values range between  $3.1 \times 10^{-6}$  and  $5.6 \times 10^{-6} \text{ s}^{-1}$ , which translates to equivalent atmospheric SOA lifetimes of 4 to 8 days with regard to photolysis in the summer, except for high- $\text{NO}_x$  toluene SOA with a lifetime of 20 days for which the effect of photolysis is likely underestimated in our simulations as discussed above. The estimated SOA lifetime with regard to photolysis is comparable or even shorter to the typical  $\sim 1$  week aerosol atmospheric lifetime which suggests that photolysis may be an important removal mechanism for atmospheric SOA. Atmospheric implications of our findings are further investigated in Sect. 3.3.

The above estimates for the  $\alpha$ -pinene SOA photolytic loss rate cannot be directly compared with those of Henry and Donahue (2012) and Wong et al. (2014) due to several factors including: (i) the differences in the chemical composition of particles as the experiments typically use the SOA pre-generated by  $\alpha$ -pinene ozonolysis for short (few hours) exposure, whereas in our simulations the SOA is generated mainly by OH oxidation, and over a much longer time period ( $> 1$  week), (ii) the possible evaporation of SOA in the laboratory experiments due to chamber heating under the UV lamps, which was not quantified in those experiments and which does not occur in our model simulations, (iii) in-particle chemistry that could modify the composition and absorption

Title Page

Abstract

Introduction

Conclusions

References

Tables

Figures

◀

▶

◀

▶

Back

Close

Full Screen / Esc

Printer-friendly Version

Interactive Discussion





**Organic photolysis reactions in tropospheric aerosols**

A. Hodzic et al.

Title Page

Abstract

Introduction

Conclusions

References

Tables

Figures



Back

Close

Full Screen / Esc

Printer-friendly Version

Interactive Discussion

figuration used in this study is described in detail by Jo et al. (2013). In particular, SOA is modeled using volatility basis set approach with aging in which oxygenated semi-volatile organic compounds (SVOC) formed by the gas-phase reaction of nine lumped hydrocarbon species (representing monoterpenes, sesquiterpenes, isoprene, and aromatic compounds) with OH, O<sub>3</sub>, and NO<sub>3</sub> are partitioned between gas and particle phases using 4 volatility bins (with saturation vapor pressures ranging from 1–1000 μg m<sup>-3</sup> at 300 K). Chemical aging of anthropogenic SVOC with OH (with a rate constant of 4 × 10<sup>-11</sup> cm<sup>3</sup> molecules<sup>-1</sup> s<sup>-1</sup>) is assumed to reduce the vapor pressure of the products by one order of magnitude. It should be noted that gas-phase photolysis of these intermediate species is not included similar to previous studies. Model simulations are performed for year 2009.

Figure 7 shows the annual mean SOA concentrations predicted by the default GEOS-Chem run within the lower troposphere (below 5 km). The predicted continental background levels of SOA typically vary between 0.2 and 0.4 μg m<sup>-3</sup>, and the highest concentrations (> 1.5 μg m<sup>-3</sup>) are found over tropical forest regions of Africa and South America. Industrialized and urban areas in China, Europe and the US feature SOA values significantly larger (0.5–1.5 μg m<sup>-3</sup>) than the background. These SOA values and spatial distribution are consistent with previous studies (e.g. Spracklen et al., 2011; Jo et al., 2013).

When the previously estimated photolytic loss of 0.04 % J<sub>NO<sub>2</sub></sub> is applied within the GEOS-Chem model, the annual mean SOA concentrations in the lower troposphere are decreased by ~ 20–30 % over source regions, and up to 60 % over remote regions. The absolute decrease is ~ 0.3 μg m<sup>-3</sup> over land and ~ 0.1 μg m<sup>-3</sup> over oceans, with the highest absolute decrease of 0.6 μg m<sup>-3</sup> coinciding with the maximum predicted SOA concentrations over Africa. As the quantum yield of the particle-phase photolysis and mass absorption coefficients are highly uncertain, here we also consider an order of magnitude higher photolytic loss rate of 0.4 % J<sub>NO<sub>2</sub></sub>. According to Fig. 7, this increase in J<sub>SOA</sub> results in a larger reduction of SOA concentrations in the lower troposphere reaching 50–70 % over land surfaces, and up to 70–90 % over water surfaces. In both

cases, a strong spatial gradient is found between land and water surfaces, with larger relative reductions in SOA concentrations over oceans. This gradient is due to the continuous photolytic losses, the effect of which accumulates further away from source regions.

Our results suggest that photolysis of SOA, which is currently ignored in chemistry-climate and air quality models, could be an efficient removal process for organic particles. The diagnosed SOA tropospheric lifetime against photolytic removal (annual-average tropospheric mass burden divided by the annual tropospheric loss due to photolysis) ranges from 1 day for  $J_{\text{SOA}} = 0.4\% J_{\text{NO}_2}$  to 7 days for  $J_{\text{SOA}} = 0.04\% J_{\text{NO}_2}$ , and is comparable to the lifetime associated with the SOA wet deposition which ranges from 3.5 to 5.5 days in these model runs. This photolytic loss pathway is expected to play a particularly important role in regions where wet deposition is not very efficient such as the upper troposphere and lower stratosphere.

## 4 Conclusions

In this study, we investigated the sensitivity of SOA formation and aging in the atmosphere to gas-phase and in-particle photolysis reactions of organic compounds that actively partition between gas and particle phases. We apply the explicit chemistry model GECKO-A to simulate SOA formation from OH oxidation of  $\alpha$ -pinene, toluene, and  $\text{C}_{12}$  and  $\text{C}_{16}$   $n$ -alkane precursors, and to explore the sensitivity of this formation to gas-phase photolysis explicitly calculated in the model. Our simulations are conducted for typical mid-latitude conditions (Boulder, CO) and a solar zenith angle of  $45^\circ$  under a week of permanent daylight. The results suggest that photolysis of intermediate organic compounds in the gas phase leads to a moderate decrease in SOA yields i.e.  $\sim 15\%$  (low- $\text{NO}_x$ ) to  $\sim 45\%$  (high- $\text{NO}_x$ ) for  $\alpha$ -pinene,  $\sim 15\%$  for toluene,  $\sim 25\%$  for  $\text{C}_{12}$   $n$ -alkane, and  $\sim 10\%$  for  $\text{C}_{16}$   $n$ -alkane during 8 days of equivalent atmospheric exposure in the summer or 3 weeks in winter. This decrease depends on the aerosol chemical composition under various  $\text{NO}_x$  levels, and the amount of photolabile molecules.

## Organic photolysis reactions in tropospheric aerosols

A. Hodzic et al.

Title Page

Abstract

Introduction

Conclusions

References

Tables

Figures



Back

Close

Full Screen / Esc

Printer-friendly Version

Interactive Discussion



SOA formed from precursors considered here contained substantial amount of photolabile molecules, many of which were partitioned to the particle-phase before they could undergo gas-phase photolysis.

We performed sensitivity studies to crudely estimate the potential effect of condensed-phase photolysis on SOA formation by either continuing to photolyze condensed-phase molecules with gas-phase rate coefficients, or by applying an equivalent  $J_{\text{SOA}}$  rate of  $4 \times 10^{-4} \times J_{\text{NO}_2} \text{ s}^{-1}$  to formed particles. The effect was comparable in terms of SOA reduction except for low- $\text{NO}_x$   $\text{C}_{16}$   $n$ -alkane SOA, for which the results suggest that photolyzed molecules further react in the gas phase and partition back to the particle phase. Our results suggest that condensed-phase photolysis might have a substantial effect on SOA formation and subsequent aging, with a decrease of 40–60% in SOA yields over ten days of equivalent atmospheric aging at mid-latitudes in the summer.

Explicit modeling of a typical  $\alpha$ -pinene ozonolysis SOA aging experiment was also performed using GECKO-A. The results show a minor decrease ( $\sim 7\%$ ) in SOA concentrations in 5 h of the aging experiment due to gas-phase photolysis of organic vapors under black UV lights. The SOA decrease is much more pronounced ( $\sim 50\%$ ) during the experiment when particle-phase photolysis was added using the gas-phase rates. The corresponding loss rate due to the combined effect of gas- and particle-phase photolysis is  $3.4 \times 10^{-5} \text{ s}^{-1}$ , which is within a factor of 2–3 of the values reported by Henry and Donahue (2012) and Wong et al. (2014).

These photolysis processes were parameterized in a global chemistry model, and the results suggest that condensed-phase photolytic reactions of organic aerosols could be an important loss process in the atmosphere, removing SOA from the troposphere on timescales of  $\sim 7$  days which is comparable to those for wet deposition. We recognize that processes occurring inside the particle-phase (e.g. oligomerization), which were not included in our study, can modify the chemical composition and properties of those chromophores, thus enhancing or reducing their ability to absorb radiation

**Organic photolysis reactions in tropospheric aerosols**

A. Hodzic et al.

Title Page

Abstract

Introduction

Conclusions

References

Tables

Figures

◀

▶

◀

▶

Back

Close

Full Screen / Esc

Printer-friendly Version

Interactive Discussion



and undergo photolysis. These reactions are still not well characterized (Atkinson and Ziemann, 2012) and are beyond the scope of this paper.

The implications of our results in terms of SOA modeling are twofold: (i) gas-phase photolysis of intermediate organic vapors which are currently ignored in most models, are likely to have a moderate impact on SOA yields over typical aerosol lifetimes in the atmosphere, (ii) in-particle photolysis could be a major sink for SOA if the quantum yields are substantial, and these need to be better constrained from measurements and included in 3-D models. It is also worth noting that a substantial sink due to in-particle photolysis would imply that our current estimates of SOA formation rates would have to be revised upwards to be consistent with observed atmospheric SOA burdens.

**The Supplement related to this article is available online at  
doi:10.5194/acpd-15-8113-2015-supplement.**

*Acknowledgements.* We thank Andrew Conley (NCAR) for help with mathematical fitting, and Albert Presto (CMU) for providing the UV lamp spectrum. This research was supported by the National Center for Atmospheric Research, which is operated by the University Corporation for Atmospheric Research on behalf of the National Science Foundation, and by DOE (BER/ASR) grant DE-SC0006711. We would like to acknowledge high-performance computing support from Yellowstone provided by NCAR's Computational and Information Systems Laboratory. Any opinions, findings and conclusions or recommendations expressed in the publication are those of the author(s) and do not necessarily reflect the views of the National Science Foundation. J. L. Jimenez was partially supported by DOE (BER/ASR) DE-SC0011105.

## References

Aumont, B., Szopa, S., and Madronich, S.: Modelling the evolution of organic carbon during its gas-phase tropospheric oxidation: development of an explicit model based on a self generating approach, *Atmos. Chem. Phys.*, 5, 2497–2517, doi:10.5194/acp-5-2497-2005, 2005.

**Organic photolysis  
reactions in  
tropospheric  
aerosols**

A. Hodzic et al.

Title Page

Abstract

Introduction

Conclusions

References

Tables

Figures



Back

Close

Full Screen / Esc

Printer-friendly Version

Interactive Discussion



**Organic photolysis  
reactions in  
tropospheric  
aerosols**

A. Hodzic et al.

Title Page

Abstract

Introduction

Conclusions

References

Tables

Figures



Back

Close

Full Screen / Esc

Printer-friendly Version

Interactive Discussion



Aumont, B., Valorso, R., Mouchel-Vallon, C., Camredon, M., Lee-Taylor, J., and Madronich, S.: Modeling SOA formation from the oxidation of intermediate volatility *n*-alkanes, *Atmos. Chem. Phys.*, 12, 7577–7589, doi:10.5194/acp-12-7577-2012, 2012.

Barnard, J. C., Volkamer, R., and Kassianov, E. I.: Estimation of the mass absorption cross section of the organic carbon component of aerosols in the Mexico City Metropolitan Area, *Atmos. Chem. Phys.*, 8, 6665–6679, doi:10.5194/acp-8-6665-2008, 2008.

Bey, I., Jacob, D. J., Yantosca, R. M., Logan, J. A., Field, B., Fiore, A. M., Li, Q., Liu, H., Mickley, L. J., and Schultz, M.: Global modeling of tropospheric chemistry with assimilated meteorology: model description and evaluation, *J. Geophys. Res.*, 106, 23073–23096, 2001.

Boucher, O., Randall, D., Artaxo, P., Bretherton, C., Feingold, G., Forster, P., Kerminen, V.-M., Kondo, Y., Liao, H., Lohmann, U., Rasch, P., Satheesh, S. K., Sherwood, S., Stevens, B., and Zhang, X. Y.: Clouds and aerosols, in: *Climate Change 2013: The Physical Science Basis. Contribution of Working Group I to the Fifth Assessment Report of the Intergovernmental Panel on Climate Change*, edited by: Stocker, T. F., Qin, D., Plattner, G.-K., Tignor, M., Allen, S. K., Boschung, J., Nauels, A., Xia, Y., Bex, V., and Midgley, P. M., Cambridge University Press, Cambridge, UK and New York, NY, USA, 2013.

Denjean, C., Formenti, P., Picquet-Varrault, B., Camredon, M., Pangui, E., Zapf, P., Katrib, Y., Giorio, C., Tapparo, A., Temime-Roussel, B., Monod, A., Aumont, B., and Doussin, J. F.: Aging of secondary organic aerosol generated from the ozonolysis of  $\alpha$ -pinene: effects of ozone, light and temperature, *Atmos. Chem. Phys.*, 15, 883–897, doi:10.5194/acp-15-883-2015, 2015.

Donahue, N. M., Henry, K. M., Mentel, T. F., Kiendler-Scharr, A., Spindler, C., Bohn, B., Brauers, T., Dorn, H. P., Fuchs, H., Tillmann, R., Wahner, A., Saathoff, H., Naumann, K. H., Möhler, O., Leisner, T., Müller, L., Reinnig, M. C., Hoffmann, T., Salo, K., Hallquist, M., Frosch, M., Bilde, M., Tritscher, T., Barmet, P., Praplan, A. P., DeCarlo, P. F., Dommen, J., Prévôt, A. S., and Baltensperger, U.: Aging of biogenic secondary organic aerosol via gas-phase OH radical reactions, *P. Natl. Acad. Sci. USA*, 21, 13503–13508, doi:10.1073/pnas.1115186109, 2012.

Epstein, S. A., Blair, S. L., and Nizkorodov, S. A.: Direct photolysis of  $\alpha$ -pinene ozonolysis secondary organic aerosol: effect on particle mass and peroxide content, *Environ. Sci. Technol.*, article ASAP, 48, 11251–11258, doi:10.1021/es502350u, 2014.



**Organic photolysis reactions in tropospheric aerosols**

A. Hodzic et al.

Title Page

Abstract

Introduction

Conclusions

References

Tables

Figures



Back

Close

Full Screen / Esc

Printer-friendly Version

Interactive Discussion



Fann, N., Lamson, A. D., Anenberg, S. C., Wesson, K., Risley, D., and Hubbell, B. J.: Estimating the national public health burden associated with exposure to ambient PM<sub>2.5</sub> and ozone, *Risk Anal.* 32, 81–95, 2012.

Finlayson-Pitts, B. J. and Pitts, J. N.: *Chemistry of the Upper and Lower Atmosphere: Theory, Experiments, and Applications*, Academic Press, San Diego, 2000.

Graber, E. R. and Rudich, Y.: Atmospheric HULIS: How humic-like are they? A comprehensive and critical review, *Atmos. Chem. Phys.*, 6, 729–753, doi:10.5194/acp-6-729-2006, 2006.

Henry, K. M. and Donahue, N. M.: Photochemical aging of  $\alpha$ -pinene secondary organic aerosol: effects of OH radical sources and photolysis, *J. Phys. Chem. A*, 116, 5932–5940, 2012.

Hodzic, A., Aumont, B., Knote, C., Lee-Taylor, J., Madronich, S., and Tyndall, G.: Volatility dependence of Henry's law constants of condensable organics: application to estimate depositional loss of secondary organic aerosols, *Geophys. Res. Lett.*, 41, 4795–4804, doi:10.1002/2014GL060649, 2014.

Jenkin, M. E., Saunders, S. M., Wagner, V., and Pilling, M. J.: Protocol for the development of the Master Chemical Mechanism, MCM v3 (Part B): tropospheric degradation of aromatic volatile organic compounds, *Atmos. Chem. Phys.*, 3, 181–193, doi:10.5194/acp-3-181-2003, 2003.

Jo, D. S., Park, R. J., Kim, M. J., and Spracklen, D. V.: Effects of chemical aging on global secondary organic aerosol using the volatility basis set approach, *Atmos. Environ.*, 81, 230–244, 2013.

Knote, C., Hodzic, A., and Jimenez, J. L.: The effect of dry and wet deposition of condensable vapors on secondary organic aerosols concentrations over the continental US, *Atmos. Chem. Phys.*, 15, 1–18, doi:10.5194/acp-15-1-2015, 2015.

Kwok, E. S. C. and Atkinson, R.: Estimation of hydroxyl radical reaction rate constants for gas-phase organic compounds using a structure–reactivity relationship: an update, *Atmos. Environ.*, 29, 1685–1695, 1995.

Lambe, E. T., Cappa, C. D., Massoli, P., Onasch, T. B., Forestieri, S. D., Martin, A. T., Cummings, M. J., Croasdale, D. R., Brune, W. H., Worsnop, D. R., and Davidovits, P.: Relationship between oxidation level and optical properties of secondary organic aerosol, *Environ. Sci. Technol.*, 47, 6349–6357, 2013.

Lignell, H., Epstein, S. A., Marvin, M. R., Shemesh, D., Gerber, B., and Nizkorodov, S.: Experimental and theoretical study of aqueous cis-pinonic acid photolysis, *J. Phys. Chem. A*, 117, 12930–12945, 2013.

**Organic photolysis  
reactions in  
tropospheric  
aerosols**

A. Hodzic et al.

Title Page

Abstract

Introduction

Conclusions

References

Tables

Figures



Back

Close

Full Screen / Esc

Printer-friendly Version

Interactive Discussion



- Madronich, S.: The atmosphere and UV-B radiation at ground level. Environmental UV Photo-  
biology, Plenum Press, 1–39, 1993.
- Nannoolal, Y., Rarey, J., and Ramjugernath, D.: Estimation of pure component properties: Part  
3. Estimation of the vapor pressure of non-electrolyte organic compounds via group contri-  
5 butions and group interactions, Fluid Phase Equilibr., 269, 117–133, 2008.
- Presto, A. A., Huff Hartz, K. E., and Donahue, N. M.: Secondary organic aerosol production  
from terpene ozonolysis. 1. Effect of UV radiation, Environ. Sci. Technol., 39, 7036–7045,  
2005.
- Salo, K., Hallquist, M., Jonsson, Å. M., Saathoff, H., Naumann, K.-H., Spindler, C., Tillmann, R.,  
10 Fuchs, H., Bohn, B., Rubach, F., Mentel, Th. F., Müller, L., Reinnig, M., Hoffmann, T., and  
Donahue, N. M.: Volatility of secondary organic aerosol during OH radical induced ageing,  
Atmos. Chem. Phys., 11, 11055–11067, doi:10.5194/acp-11-11055-2011, 2011.
- Schilling-Fahnestock, K. A., Yee, L. D., Loza, C. L., Coggon, M. M., Schwantes, R., Zhang, X.,  
Dalleska, N. F., and Seinfeld, J. H.: Secondary organic aerosol composition from C12 alka-  
15 nes, J. Phys. Chem. A, doi:10.1021/jp501779w, 2014.
- Spracklen, D. V., Jimenez, J. L., Carslaw, K. S., Worsnop, D. R., Evans, M. J., Mann, G. W.,  
Zhang, Q., Canagaratna, M. R., Allan, J., Coe, H., McFiggans, G., Rap, A., and Forster, P.:  
Aerosol mass spectrometer constraint on the global secondary organic aerosol budget, At-  
mos. Chem. Phys., 11, 12109–12136, doi:10.5194/acp-11-12109-2011, 2011.
- 20 Tritscher, T., Dommen, J., DeCarlo, P. F., Gysel, M., Barmet, P. B., Praplan, A. P., Weingart-  
ner, E., Prévôt, A. S. H., Riipinen, I., Donahue, N. M., and Baltensperger, U.: Volatility and  
hygroscopicity of aging secondary organic aerosol in a smog chamber, Atmos. Chem. Phys.,  
11, 11477–11496, doi:10.5194/acp-11-11477-2011, 2011.
- Wong, J. P. S., Zhou, S., and Abbatt, P. D.: Changes in secondary organic aerosol composition  
25 and mass due to photolysis: relative humidity dependence, J. Phys. Chem. A, article ASAP,  
doi:10.1021/jp506898c, 2014.
- Yee, L. D., Craven, J. S., Loza, C. L., Schilling, K. A., Ng, N. L., Canagaratna, M. R., Zie-  
mann, P. J., Flagan, R. C., and Seinfeld, J. H.: Secondary organic aerosol formation from  
low-NO<sub>x</sub> photooxidation of dodecane: evolution of multigeneration gas-phase chemistry and  
aerosol composition, J. Phys. Chem. A, 116, 6211–6230, doi:10.1021/jp211531h, 2012.
- 30 Zhang, J., Hartz, K. E. H., Pandis, S. N., and Dohanue, N. M.: Secondary organic aerosol for-  
mation from limonene ozonolysis: homogeneous and heterogeneous influences as a function  
of NO<sub>x</sub>, J. Phys. Chem. A, 110, 11053–11063, 2006.

Ziemann, P. J. and Atkinson, R.: Kinetics, products, and mechanism of secondary organic aerosol formation, Chem. Soc. Rev., 41, 6582–6605, 2012.

ACPD

15, 8113–8149, 2015

**Organic photolysis reactions in tropospheric aerosols**

A. Hodzic et al.

Title Page

Abstract

Introduction

Conclusions

References

Tables

Figures



Back

Close

Full Screen / Esc

Printer-friendly Version

Interactive Discussion



## Organic photolysis reactions in tropospheric aerosols

A. Hodzic et al.

Title Page

Abstract

Introduction

Conclusions

References

Tables

Figures

◀

▶

◀

▶

Back

Close

Full Screen / Esc

Printer-friendly Version

Interactive Discussion

**Table 1.** Photolysis rate coefficients and photolytic lifetimes for typical atmospheric conditions and for our simulations.

Typical conditions		Average $J_{\text{NO}_2}$ ( $\text{s}^{-1}$ )	$J_{\text{NO}_3}$ exposure (lifetimes) in 1 day*	Average $J_{\text{O}_1\text{D}}$ ( $\text{s}^{-1}$ )	$J_{\text{O}_1\text{D}}$ exposure (lifetimes) in 1 day	Average $J_{\text{NO}_3 \rightarrow \text{NO}_2 + \text{O}}$ ( $\text{s}^{-1}$ )	$J_{\text{NO}_3}$ exposure (lifetimes) in 1 day
Boulder CO, summer solstice	40° N, sea level, 21 Jun, $\text{O}_{3\text{col.}} = 310$ DU, 10% ground albedo, no aerosols, no clouds	$4.1 \times 10^{-3}$	354	$1.0 \times 10^{-5}$	0.96	$9.1 \times 10^{-2}$	$7.9 \times 10^3$
Boulder CO, winter solstice	40° N, sea level, 21 Dec, $\text{O}_{3\text{col.}} = 330$ DU, 10% ground albedo, no aerosols, no clouds	$1.5 \times 10^{-3}$	130	$1.2 \times 10^{-6}$	0.1	$4.6 \times 10^{-2}$	$4.0 \times 10^3$
Equator 21 Jun	Sea level, $\text{O}_{3\text{col.}} = 260$ DU, 5% ground albedo, no aerosols, no clouds	$3.3 \times 10^{-3}$	285	$1.0 \times 10^{-5}$	0.86	$7.3 \times 10^{-2}$	$6.3 \times 10^3$
Equator 21 Mar	Sea level, $\text{O}_{3\text{col.}} = 258$ DU, 5% ground albedo, no aerosols, no clouds	$3.6 \times 10^{-3}$	311	$1.3 \times 10^{-5}$	1.1	$7.8 \times 10^{-2}$	$6.7 \times 10^3$
Hyytiälä, summer solstice	61° N, 21 Jun, $\text{O}_{3\text{col.}} = 355$ DU, 5% ground albedo, no aerosols, no clouds	$4.3 \times 10^{-3}$	372	$6.2 \times 10^{-6}$	0.54	$1.0 \times 10^{-1}$	$8.6 \times 10^3$
Hyytiälä, winter solstice	61° N, 21 Dec, $\text{O}_{3\text{col.}} = 355$ DU, 9% ground albedo, no aerosols, no clouds	$2.6 \times 10^{-4}$	22	$5.8 \times 10^{-8}$	$4.8 \times 10^{-3}$	$1.0 \times 10^{-2}$	$8.6 \times 10^2$

\*  $J_{\text{NO}_2}$  1 day exposure is calculated as  $J_{\text{NO}_2} \times 86\,400$  (in s).

## Organic photolysis reactions in tropospheric aerosols

A. Hodzic et al.

Title Page

Abstract

Introduction

Conclusions

References

Tables

Figures



Back

Close

Full Screen / Esc

Printer-friendly Version

Interactive Discussion



Table 1. Continued.

Model simulation		Average $J_{\text{NO}_2}$ ( $\text{s}^{-1}$ )	Average $J_{\text{O}_1\text{D}}$ ( $\text{s}^{-1}$ )	Average $J_{\text{NO}_3 \rightarrow \text{NO}_2 + \text{O}}$ ( $\text{s}^{-1}$ )	Photolysis Age in $J_{\text{NO}_2}$ equivalent days	
					Boulder, CO summer solstice	Boulder, CO winter solstice
GECKO-A 1 week simulations (Table 2)	40° N, 45° solar zenith angle, 7 days	$8.1 \times 10^{-3}$	$2.1 \times 10^{-5}$	$1.8 \times 10^{-1}$	14 eq. days	38 eq. days
GECKO-A $\alpha$ -pinene ozonolysis SOA (Fig. 6)	Black lights, 5 h	$3.0 \times 10^{-3}$	$1.2 \times 10^{-5}$	$2.1 \times 10^{-3}$	0.15 eq. days (3.7 eq. h)	0.42 eq. days (10 eq. h)
Henry and Donahue (2012)	Black lights, 5 h	$3.0 \times 10^{-3}$	–	–	0.15 eq. days (3.7 eq. h)	0.42 eq. days (10 eq. h)

## Organic photolysis reactions in tropospheric aerosols

A. Hodzic et al.

Title Page

Abstract

Introduction

Conclusions

References

Tables

Figures

◀

▶

◀

▶

Back

Close

Full Screen / Esc

Printer-friendly Version

Interactive Discussion

**Table 2.** Description of GECKO-A simulations.

Experiments for SOA formed from $\alpha$ -pinene, toluene, C <sub>12</sub> , C <sub>16</sub> <i>n</i> -alkane				
	Gas-phase photolysis of organics	Particle-phase photolysis	OH (molecules cm <sup>-3</sup> )	OA back-ground (μg m <sup>-3</sup> )
BASE	ON/OFF	OFF	$2 \times 10^6$	10
SENS_OA	ON/OFF	OFF	$2 \times 10^6$	1
SENS_OH	ON/OFF	OFF	$8 \times 10^6$	1
$J_{\text{molecmax}}$	ON	ON as gas-phase $J$	$2 \times 10^6$	10
$J_{\text{molec}}$	ON	ON as gas-phase $J$ and further gas-phase chemistry of products of photolysis	$2 \times 10^6$	10
$J_{\text{mac}}$	ON	ON as 0.04 % $J_{\text{NO}_2}$	$2 \times 10^6$	10

## Organic photolysis reactions in tropospheric aerosols

A. Hodzic et al.

**Table 3.** Predicted reduction in SOA yields due to gas-phase photolysis, and corresponding first order loss rates and lifetimes. The results are from the GECKO-A BASE case simulation, and yields values are taken at the maximum of the SOA formation from each precursor. The loss rate coefficients were estimated by numerically fitting the first order decay of SOA due to photolysis occurring over one week of processing at constant light ( $J_{\text{NO}_2} = 8.1 \times 10^{-3} \text{ s}^{-1}$ ). Low (0.01 ppb) and high (10 ppb)  $\text{NO}_x$  simulations are shown.

Considered System	Reduction in SOA yields by gas-phase photolysis		Estimated loss rate ( $\text{s}^{-1}$ )		Estimated lifetime (days, under simulation conditions*)	
	Low $\text{NO}_x$	High $\text{NO}_x$	Low $\text{NO}_x$	High $\text{NO}_x$	Low $\text{NO}_x$	High $\text{NO}_x$
$\alpha$ -pinene + OH	−16 %	−47 %	$4.6 \times 10^{-7}$	$2.1 \times 10^{-6}$	25.0	5.4
Toluene + OH	−11 %	−13 %	$5.6 \times 10^{-7}$	$4.3 \times 10^{-7}$	20.8	27.0
$\text{C}_{12}\text{H}_{26}$ + OH	−30 %	−28 %	$1.2 \times 10^{-6}$	$1.1 \times 10^{-6}$	9.3	10.4
$\text{C}_{16}\text{H}_{34}$ + OH	−10 %	−13 %	$3.6 \times 10^{-7}$	$3.7 \times 10^{-7}$	30.0	31.0

\* To derive equivalent atmospheric loss rates (lifetimes) at mid-latitudes values should be divided (multiplied) by a factor of 2 in summer and 5.4 in winter which is the ratio between  $J_{\text{NO}_2}$  used in our experiment and the typical atmospheric values.

Title Page

Abstract

Introduction

Conclusions

References

Tables

Figures

◀

▶

◀

▶

Back

Close

Full Screen / Esc

Printer-friendly Version

Interactive Discussion





## Organic photolysis reactions in tropospheric aerosols

A. Hodzic et al.

**Table 4.** Estimated loss rates and lifetimes due to gas-phase and in-particle phase photolysis as predicted by GECKO-A for the  $J_{\text{mac}}$  simulation over one week of aging at constant light ( $J_{\text{NO}_2} = 8.1 \times 10^{-3} \text{ s}^{-1}$ ).

Considered System	Estimated loss rate ( $\text{s}^{-1}$ )		Estimated lifetime (days, under simulation conditions)	
	Low $\text{NO}_x$	High $\text{NO}_x$	Low $\text{NO}_x$	High $\text{NO}_x$
$\alpha$ -pinene + OH	$3.7 \times 10^{-6}$	$5.6 \times 10^{-6}$	3.1	2.1
Toluene + OH	$3.1 \times 10^{-6}$	$1.1 \times 10^{-6}$	3.7	10.5
$\text{C}_{12}\text{H}_{26}$ + OH	$4.7 \times 10^{-6}$	$4.4 \times 10^{-6}$	2.5	2.6
$\text{C}_{16}\text{H}_{34}$ + OH	$3.7 \times 10^{-6}$	$3.5 \times 10^{-6}$	3.1	3.3

\* To derive equivalent atmospheric loss rates (lifetimes) at mid-latitudes values should be divided (multiplied) by a factor of 2 in summer and 5.4 in winter which is the ratio between  $J_{\text{NO}_2}$  used in our experiment and the typical atmospheric values.

Title Page

Abstract

Introduction

Conclusions

References

Tables

Figures

◀

▶

◀

▶

Back

Close

Full Screen / Esc

Printer-friendly Version

Interactive Discussion



## Organic photolysis reactions in tropospheric aerosols

A. Hodzic et al.

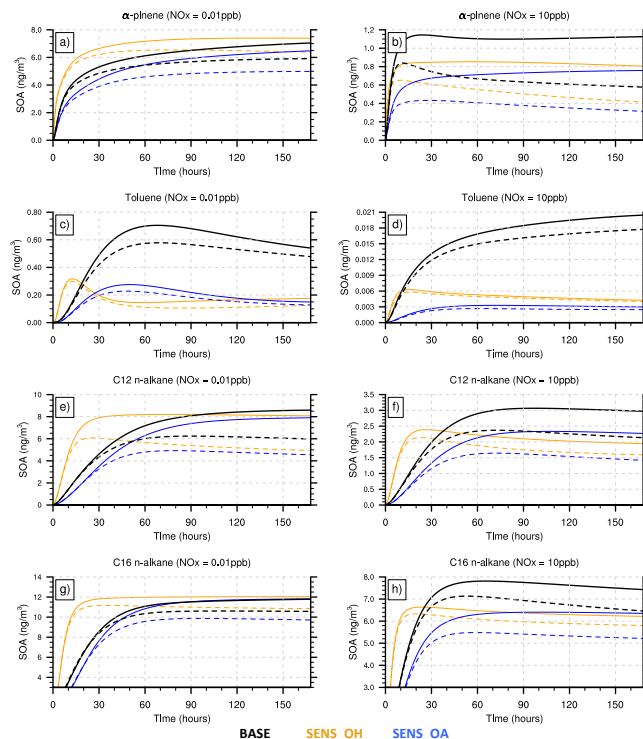


**Figure 1.** SOA formation from the oxidation by OH of 1 ppt of  $\alpha$ -pinene, toluene, C<sub>12</sub> and C<sub>16</sub> *n*-alkanes at low (0.01 ppb) and high (10 ppb) NO<sub>x</sub> levels. Plots compare GECKO-A simulations with (dashed lines) and without (full lines) gas-phase photolysis of organics at the solar zenith angle of 45° (mid-latitudes) at constant daylight. To derive equivalent atmospheric summertime exposure of our experiment, the time axes should be multiplied by a factor of 2 (see Table 1). Reference simulation (BASE) is shown in black, and is compared to two sensitivity simulations testing for higher OH levels (SENS\_OH in orange) and lower absorbing organic aerosol mass (SENS\_OA in blue). See Table 2 for the description of various runs.

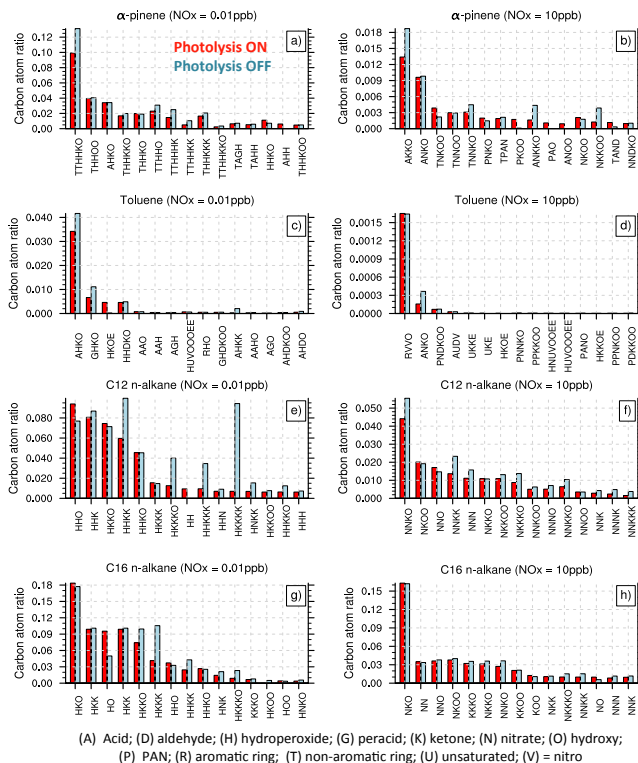


**Figure 2.** Particle-phase dominant functional groups in the top fifteen SOA constituents shown at the maximum of the SOA yield. The BASE case simulations with (red bars) and without (blue bars) photolysis of organic compounds are compared.

## Organic photolysis reactions in tropospheric aerosols

A. Hodzic et al.

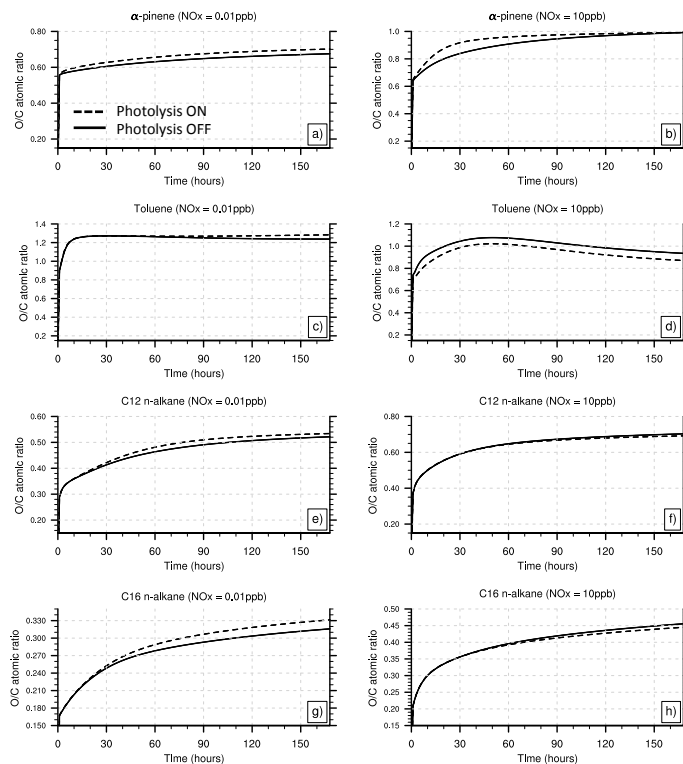


**Figure 3.** Oxygen to carbon (O/C) ratios as predicted by the BASE case simulation with (dashed lines) and without (full lines) gas-phase photolysis of organics.

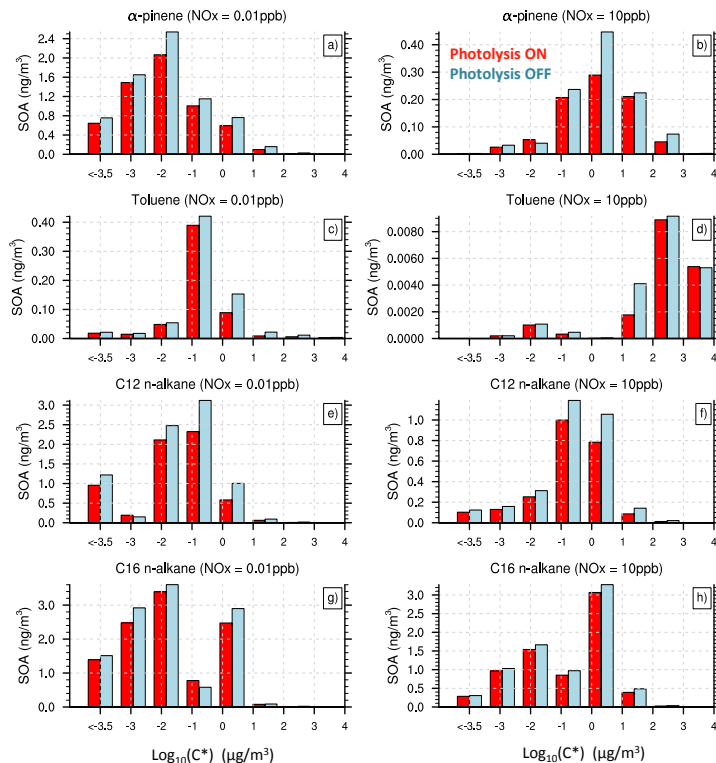


**Figure 4.** Volatility distribution of products of OH oxidation of 1 ppt of  $\alpha$ -pinene, toluene, C<sub>12</sub> and C<sub>16</sub> *n*-alkanes at low (0.01 ppb) and high (10 ppb) NO<sub>x</sub> levels. Predictions represent values at the maximum SOA yield based on the BASE case simulation with (red) and without (blue) gas-phase photolysis of organics.

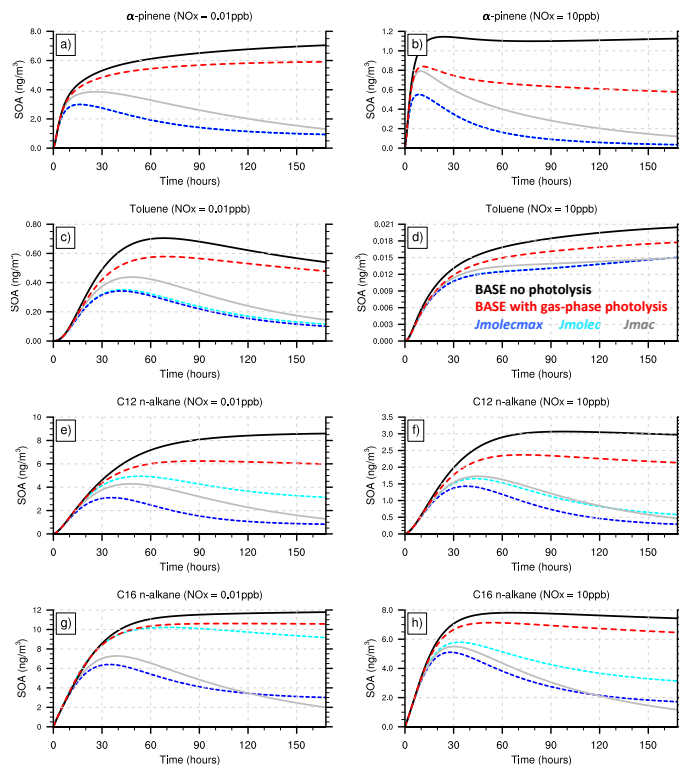


**Figure 5.** Predicted effect of photolysis on SOA formation from the oxidation of 1 ppt of  $\alpha$ -pinene, toluene, C<sub>12</sub> and C<sub>16</sub> *n*-alkanes at low (0.01 ppb) and high (10 ppb) NO<sub>x</sub> levels. Plots compare GECKO-A simulations for the BASE no photolysis run (black), BASE run with gas-phase photolysis (red),  $J_{molecmax}$  (blue),  $J_{molec}$  (cyan) and  $J_{mac}$  (gray). To derive equivalent atmospheric summertime exposure of our experiments, times should be multiplied by a factor of 2 (Table 1). See Table 2 for the description of various runs.

## Organic photolysis reactions in tropospheric aerosols

A. Hodzic et al.

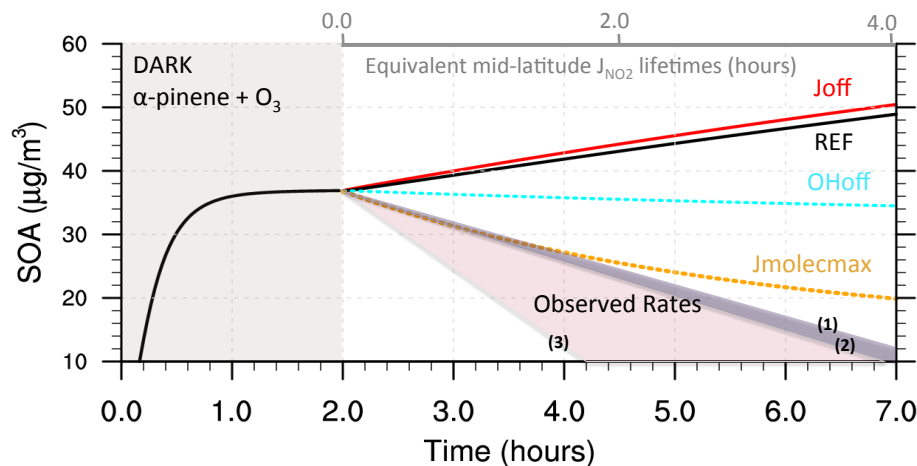


**Figure 6.** GECKO-A simulation of a typical SOA aging experiment. SOA is first made in the dark in 2 h from  $\alpha$ -pinene ozonolysis in the conditions where the formation of hydroperoxides dominates (through  $\text{RO}_2 + \text{HO}_2$  reactions). After the 2nd hour the initial precursor has been consumed, and the SOA mixture is exposed to various conditions: (REF, black) UV black lights and OH of  $10^6 \text{ molecules cm}^{-3}$ ; ( $J_{\text{off}}$ , red) only OH oxidation with  $\text{OH} = 10^6 \text{ molecules cm}^{-3}$  and photolysis are turned off for organic compounds; ( $\text{OH}_{\text{off}}$ , cyan blue) only UV black lights; ( $J_{\text{molecmax}}$ , orange) similar to the REF case, but the photolysis of organic molecules is performed also in the condensed phase. The UV lamp is that of Presto et al. (2005), with  $J_{\text{NO}_2} = 3 \times 10^{-3} \text{ s}^{-1}$ ,  $\text{NO}_x$  levels are kept at 0.01 ppb, and ozone levels are set at 50 ppb during the aging simulations. SOA loss rates reported in the experiments are also shown in shaded purple areas with slopes corresponding to (1) Henry and Donahue (2012) ( $6 \times 10^{-5} \text{ s}^{-1}$ ), (2) Wong et al. (2014) for dry conditions ( $7.9 \times 10^{-5} \text{ s}^{-1}$ ) and (3) Wong et al. (2014) for humid conditions ( $1.6 \times 10^{-4} \text{ s}^{-1}$ ).

## Organic photolysis reactions in tropospheric aerosols

A. Hodzic et al.

Title Page

Abstract

Introduction

Conclusions

References

Tables

Figures



Back

Close

Full Screen / Esc

Printer-friendly Version

Interactive Discussion

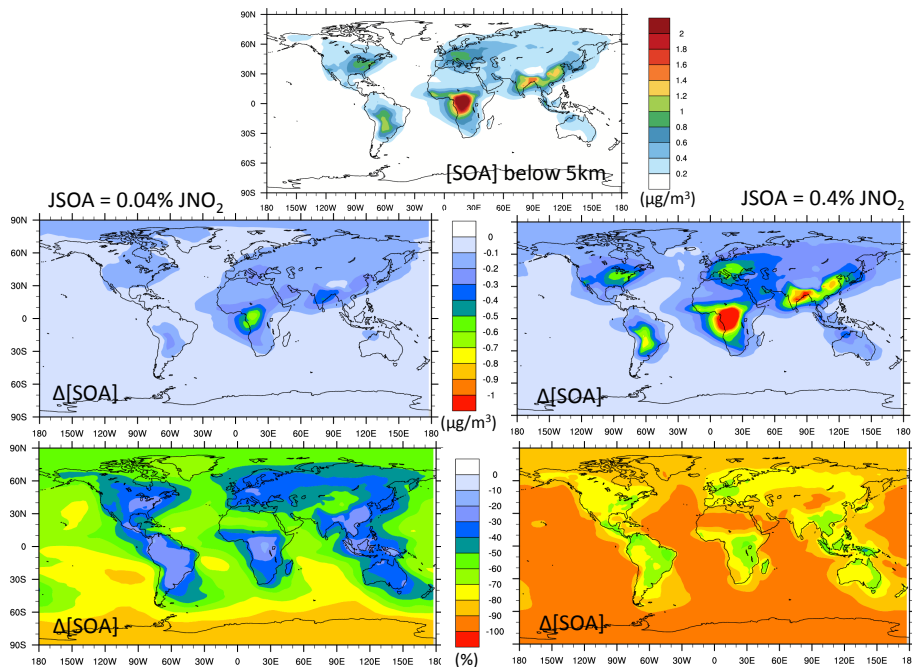


**Figure 7.** GEOS-Chem simulation for 2009 showing the absolute ( $\mu\text{g m}^{-3}$ ) and relative (%) reductions in SOA concentrations within the lower troposphere (below 5 km). Two photolysis rates are considered i.e.  $J_{\text{SOA}}$  of 0.04 %  $J_{\text{NO}_2}$  (left plots), and  $J_{\text{SOA}}$  of 0.4 %  $J_{\text{NO}_2}$  (right plots).